CODEN STJSAO
ZX470/1476

ISSN 0562-1887
UDK 536.24:536.629.7 :519.61/.64

Heat Transfer Analysis of Heating Plate with Multiple Heat Sources

Paolo BLECICH, Kristian LENIĆ, Anica TRP* and *Bernard FRANKOVIĆ

Tehnički fakultet Sveučilišta u Rijeci
(Faculty of Engineering, University of Rijeka),
Vukovarska 58, HR-51000 Rijeka,
Republic of Croatia

paolo.blecich@riteh.hr

Keywords
Heat sources depth
Heating plate
Infrared camera
Numerical analysis
Thermal diffusivity

Ključne riječi
Dubina izvora topline
Grijaća ploča
Infracrvena kamera
Numerička analiza
Temperaturna vodljivost

Received (primljeno): 2009-04-30
Accepted (prihvaćeno): 2010-06-30

Preliminary note

3D numerical study of transient heat transfer phenomenon on a solid plate with complex heat sources has been carried out. In order to validate the chosen numerical model, a set of thermographic measurements have been performed on a heating plate sample. The infrared camera provided a number of thermograms showing the development of transient temperature fields on the plate surface. Satisfactory agreement between thermograms and numerically obtained temperature fields has been achieved. Based upon the validated numerical model, an approach involving thermographic measurements has been used to estimate the position of heat sources inside the plate. Numerically obtained temperature distributions have been used for calculation of effective transient heating output. The unsteady behavior of the heating plate with complex heat sources has been numerically studied for different plate materials. It has been concluded that the temperature fields and transient heating outputs depend on physical properties of the plate material. However, when a steady state has been achieved, different plate materials give equivalent steady heating outputs despite different temperature distributions.

Analiza prijelaza topline unutar grijaće ploče s mnogostrukim izvorima topline

Prethodno priopćenje

Provedena je 3D numerička analiza nestacionarnog prijelaza topline u grijaćoj ploči s mnogostrukim izvorima topline. Valjanost odabranog numeričkog modela provjerena je usporedbom s termografskim snimcima koji su načinjeni na uzorku grijaće ploče. Infracrvena je kamera osigurala dovoljan broj termograma koji prikazuju nestacionarne temperaturne raspodjele na površini ploče. Usporedbom termograma i numeričkim putem dobivenih temperaturnih raspodjela utvrđena je dobra podudarnost termografskih mjerenja i numeričkih simulacija. Temeljeći se na provjerenom numeričkom modelu, razvijen je postupak za određivanje položaja izvora topline u grijaćoj ploči pomoću termografskih mjerenja. Numeričkim putem dobivene temperaturne raspodjele na površini ploče korištene su za određivanje toplinskog učina grijaće ploče. Nestacionarno ponašanje temperaturnih raspodjela na grijaćoj ploči s mnogostrukim izvorima topline ispitivano je numeričkim putem za različite materijale ploče. Zaključeno je da raspodjele temperatura i nestacionarni toplinski učini ovise o fizikalnim svojstvima materijala ploče. Međutim, kada se postigne stacionarno stanje, različiti materijali ploče daju jednake toplinske učinke usprkos različitim temperaturnim raspodjelama.

1. Introduction

The main objective of this work was to get an image of the relationship between material physical properties and the temperature distributions at the surface for solid materials with complex internal heat sources.

Generally speaking, physical properties such as thermal conductivity λ, density ρ and specific heat capacity c dictate the speed of heat diffusion throughout a solid. The thermal conductivity expresses the ability of a material to conduct heat. On the other hand, the product of density and specific heat capacity, represents the heat storage capability of a material. All together, these properties are gathered to yield the thermal diffusivity of a material

$$a = \frac{\lambda}{\rho\, c}. \tag{1}$$

Therefore, the thermal diffusivity is the ratio of conducted heat to the stored heat in a solid and the larger the thermal diffusivity, the faster the heat diffusion through the solid.

It will be shown that temperature distributions on the body surface depend on the rate of heat diffusion through

Symbols/Oznake

a	- thermal diffusivity, m^2/s - koef. temperaturne vodljivosti	α	- heat transfer coefficient, W/m^2K - koeficijent prijelaza topline
c	- specific heat capacity, J/kg·K - specifični toplinski kapacitet	δ	- heat sources depth, m - dubina izvora topline
H	- height, m - visina	ε	- emissivity - emisijski faktor
L	- length, m - duljina	λ	- thermal conductivity, W/m·K - koef. toplinske vodljivosti
$\dot{q}$	- heat source heating rate, W/m^3 - učin izvora topline	υ	- kinematic viscosity, m^2/s - kinematska žilavost
B	- thickness, m - debljina	ϑ	- temperature, K - temperature
t	- time, s - vrijeme	ρ	- mass density, kg/m^3 - gustoća
x, y, z	- coordinate axis - koordinatne osi	σ	- blackbody constant, W/m^2K^4 - konstanta zračenja crnog tijela

the body. A material with large thermal diffusivity (e.g. aluminium, copper, steel) transfers heat at a higher rate than a material with low thermal diffusivity (e.g. wood, plastics) and thus the temperature fields are more uniformly disposed on the surface [1-2].

The above-mentioned analysis has been carried out for a heating plate of 100×40×3 cm dimensions with complex internal heat sources. The heat sources were electric resistances with a constant heating rate. The development of transient temperature fields were recorded by means of an infrared (IR) camera and subsequently numerically analyzed [3]. The IR camera is a modern engineering measuring device, largely used for control, maintenance and diagnosis demands, capable of generating thermograms up to 640 × 480 pixels.

2. Mathematical model

2.1. Domain

Although contemporary software offers a large number of different approaches and numerical models for the governing equations to be solved, the user must be always and fully aware of the theoretical basis concerning the nature of the problem. Therefore, a brief description of the domain, governing equations and boundary conditions has been given. The domain is a stone heating plate with electric wire-heaters placed inside the plate, shown in Figure 1. The properties of the stone heating plate are given in Table 1.

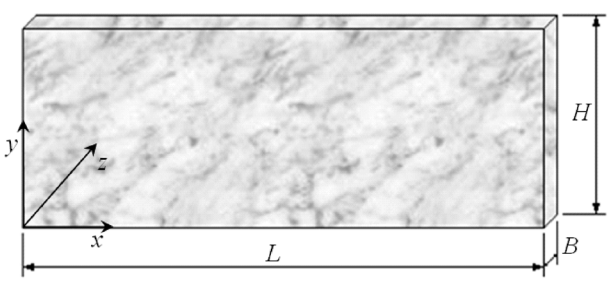

Figure 1. Domain dimensions

Slika 1. Dimenzije domene

Table 1. Heating plate properties

Tablica 1. Karakteristike grijaće ploče

Heating output/Toplinski učin	800 W
Heat sources heating power/ Toplinski učinak izvora topline	66.7 W/m
Dimensions/Dimenzije:	
Length/Duljina, L	1000 mm
Height/Visina, H	400 mm
Thickness/Debljina, B	30 mm
Material/Materijal	Stone/Kamen -Bračko veselje
Density/Gustoća	2600 kg/m^3
Thermal conductivity/ Koef. toplinske vodljivosti	2.8 W/mK
Specific heat capacity/ Specifični toplinski kapacitet	810 J/kg·K
Thermal diffusivity/ Koef. temperaturne vodljivosti	1.33 mm^2/s

2.2. Governing equations

The governing equation describing the heat conduction in a solid, in its most general form, is the transient three-dimensional heat conduction equation

$$\rho\, c\frac{\partial \vartheta}{\partial t}=\frac{\partial}{\partial x}\left(\lambda\frac{\partial \vartheta}{\partial x}\right)+\frac{\partial}{\partial y}\left(\lambda\frac{\partial \vartheta}{\partial y}\right)+\frac{\partial}{\partial z}\left(\lambda\frac{\partial \vartheta}{\partial z}\right)+\dot{q}_{\mathrm{v}}, \quad (2)$$

where $\dot{q}_{\mathrm{v}}$ is the source term. For isotropic heating plate material i.e. λ = const., equation (2) can be rewritten as

$$\frac{\partial \vartheta}{\partial t}=a\left(\frac{\partial^2 \vartheta}{\partial x^2}+\frac{\partial^2 \vartheta}{\partial y^2}+\frac{\partial^2 \vartheta}{\partial z^2}\right)+\frac{\dot{q}_{\mathrm{v}}}{\rho\, c}. \quad (3)$$

2.3. Initial and boundary conditions

The initial condition expresses the temperature distribution of the heating plate at the beginning of the analysis. Before turning on the electric heat sources, it is supposed that the plate is at uniform temperature ϑ_0 hence

$$\vartheta(x,y,z,t=0)=\vartheta_0. \quad (4)$$

The boundary conditions are of the third kind, which corresponds to the existence of mixed convection-radiation heat transfer at the plate surfaces [4]. According to Figure 1 the boundary conditions can be written as:

x - axis: for $x = 0$, $0 \le y \le H$, $0 \le z \le B$,

$$-\lambda\left.\frac{\partial \vartheta}{\partial x}\right|_{x=0}=\alpha\left[\vartheta_\infty-\vartheta(0,y,z,t)\right],$$

for $x = L$, $0 \le y \le H$, $0 \le z \le B$,

$$-\lambda\left.\frac{\partial \vartheta}{\partial x}\right|_{x=L}=\alpha\left[\vartheta_\infty-\vartheta(L,y,z,t)\right],$$

y - axis: $0 \le x \le L$, $y = 0$, $0 \le z \le B$,

$$-\lambda\left.\frac{\partial \vartheta}{\partial y}\right|_{y=0}=\alpha\left[\vartheta_\infty-\vartheta(x,0,z,t)\right],$$

for $0 \le x \le L$, $y = H$, $0 \le z \le B$,

$$-\lambda\left.\frac{\partial \vartheta}{\partial y}\right|_{y=H}=\alpha\left[\vartheta_\infty-\vartheta(x,H,z,t)\right],$$

z - axis: for $0 \le x \le L$, $0 \le y \le H$, $z = 0$,

$$-\lambda\left.\frac{\partial \vartheta}{\partial z}\right|_{z=0}=\alpha\left[\vartheta_\infty-\vartheta(x,y,0,t)\right],$$

for $0 \le x \le L$, $0 \le y \le H$, $z = B$,

$$-\lambda\left.\frac{\partial \vartheta}{\partial z}\right|_{z=B}=\alpha\left[\vartheta_\infty-\vartheta(x,y,B,t)\right].$$

The overall heat transfer coefficient α consists of a convective α_{c} and a radiative α_{r} part. Using the average values of the coefficients gives

$$\bar{\alpha}=\bar{\alpha}_{\mathrm{c}}+\bar{\alpha}_{\mathrm{r}}. \quad (5)$$

The average convection heat transfer coefficient is determined as

$$\bar{\alpha}_{\mathrm{c}}=0.59\frac{\lambda}{H}\left[\frac{H^3 g(\vartheta-\vartheta_\infty)}{\nu^2\vartheta_\infty}\frac{\nu}{a}\right]^{0.25}, \quad (6)$$

while the average radiation heat transfer coefficient is

$$\bar{\alpha}_{\mathrm{r}}=\frac{\varepsilon\cdot\sigma\left[\vartheta^4-\vartheta_{\mathrm{s}}^4\right]}{\vartheta-\vartheta_\infty}, \quad (7)$$

where ϑ is the average surface temperature of the heating plate, obtained from thermograms or numerical calculations, ϑ_{s} and ϑ_∞ are the temperatures of the surrounding surfaces and the room air temperature, respectively.

The boundary condition at the heater-material interface is a boundary condition of the second kind as shown in Figure 2, i.e. a constant surface heat flux is assumed

$$-\lambda\left.\frac{\partial \vartheta}{\partial r}\right|_{r=R}=\dot{q}_{\mathrm{s}}. \quad (8)$$

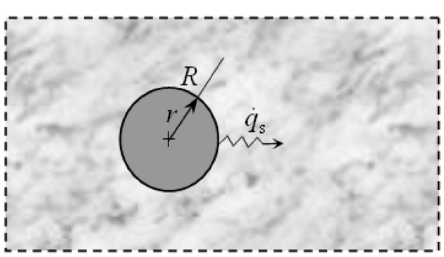

Figure 2. Constant heat flux at the heater-material interface

Slika 2. Konstantan toplinski tok na dodirnoj površini grijač-materijal

3. Numerical calculations

Using the finite volume method the domain and the related heat conduction equation (3) have been discretized and solved for a finite number of nodes marching along the time coordinate [5-7].

A fully implicit method has been used for time-stepping treatment. The domain has been meshed using *Gambit* and numerically solved using *Fluent* software.

4. Experimental setup and validation

Temperature distributions on the surface of the heating plate have been recorded by an IR camera. The experimental setup is shown in Figure 3.

The used IR camera is a LWIR sensitive, 320×240 array size uncooled microbolometer detector camera, model ThermaCAM S65 – FLIR Systems [8], owned by the Laboratory for Thermal Measurements of the Faculty of Engineering, University of Rijeka.

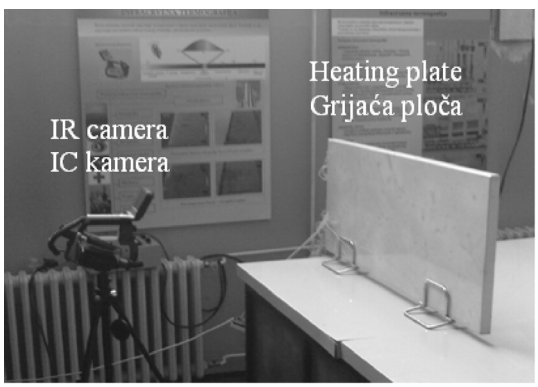

Figure 3. The experimental setup

Slika 3. Mjerna linija

Measurements were performed at ambient temperature of 18 °C. Calibration of the heating plate surface emissivity, input value for the IR camera, was performed measuring the surface temperature. The measured emissivity is $\varepsilon = 0.94$

Thermographic and numerically obtained temperature fields have been compared until a steady state was reached: the results are shown as plots of average, minimum and maximum temperature in Figure 4.

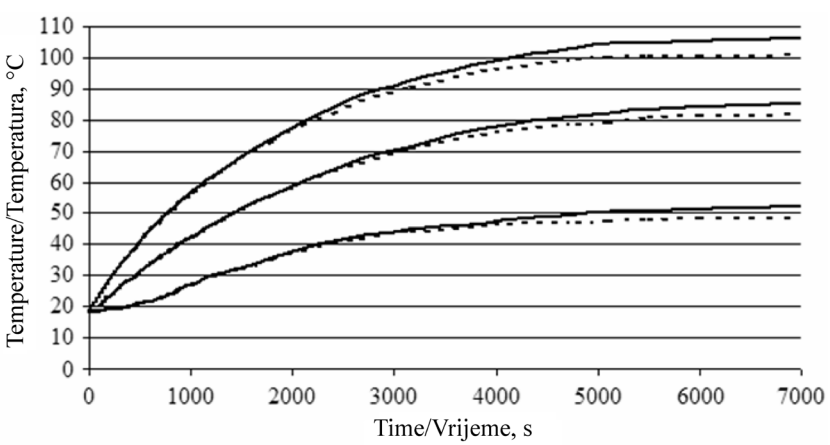

Figure 4. Average, minimum and maximum temperature of the heating plate, resulting from thermograms (solid line) and from computational analysis (dashed line), as a function of time

Slika 4. Prosječna, minimalna i maksimalna temperatura grijaće ploče, dobivena pomoću termografskih snimaka (puna linija) i računalnih analiza (isprekidana linija), u funkciji vremena

Satisfactory agreement between recorded thermograms and numerically obtained temperature fields of the heating plate has been achieved. Although increasing deviations in time between experimental and numerical temperature plots suggest an underestimated heat flux at the heater-material interface, the maximum error does not exceed 7 %.

Numerically obtained temperature distribution and a thermogram of the heating plate for the time moment of 3600 s are shown in Figure 5.

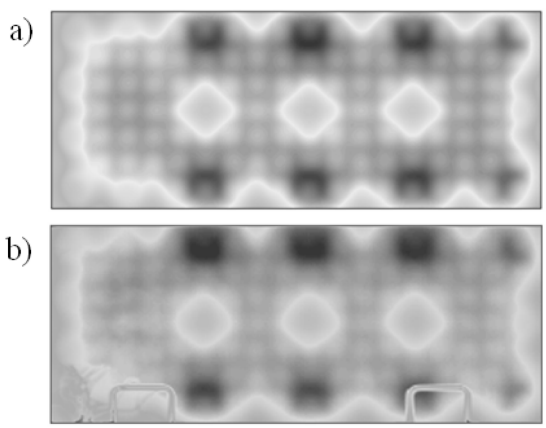

Figure 5. Temperature distributions of the heating plate at time moment $t = 3600$ s obtained a) numerically and b) by IR camera

Slika 5. Raspodjele temperatura na grijaćoj ploči u vremenskom trenutku $t = 3600$ s dobivene a) numeričkim putem i b) IC kamerom

Since satisfactory agreement between thermograms and numerically obtained temperature fields has been achieved, the numerical model is validated.

5. Results of the analysis

5.1. Temperature fields

The electric heaters are embedded in a double passage (dark-gray colour) near the upper and the lower edge of the plate, whilst in the central area there are three zones without heaters as shown in Figure 6. In the remaining parts of the plate, heaters are found to be posted equally in a honeycomb pattern (light-gray colour). Such a choice is conditioned by the fact that using stronger heating at the edges with respect to the central area, non-uniform heating of the

plate material is balanced to prevent its possible cracking under thermal stress.

Figure 7 shows the time-developing temperature fields on the heating plate at four different time moments.

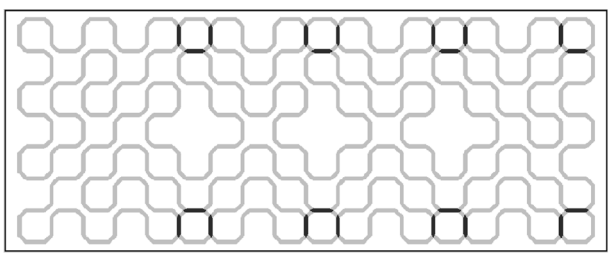

Figure 6. Location of heat sources inside the heating plate

Slika 6. Položaj izvora topline unutar grijaće ploče

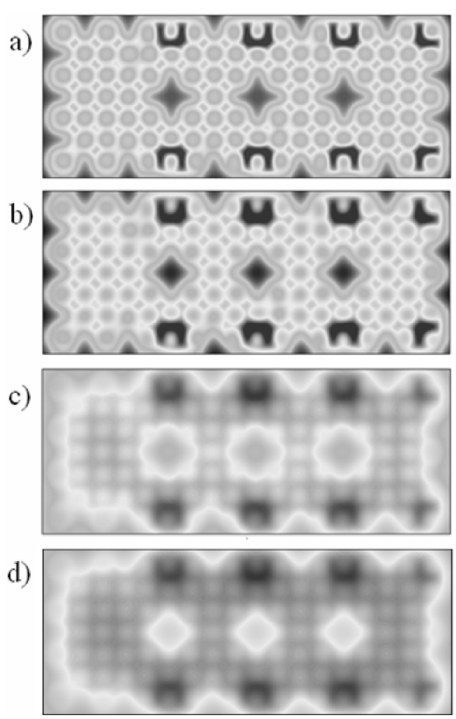

Figure 7. Numerically obtained temperature distributions of the heating plate at: a) 120 s, b) 300 s, c) 2400 s and d) 5400 s. The heat sources depth is 12.5 mm.

Slika 7. Numeričkim putem dobivene temperaturne raspodjele za: a) 120 s, b) 300 s, c) 2400 s i d) 5400 s. Dubina izvora topline je 12,5 mm

5.2. Steady-state achievement and heat sources depth

Steady state is reached when the heat flux coming from the heat sources becomes equal to the heat flux leaving the plate surface, either by convection or radiation. Steady state is assumed to occur when the growth of maximum temperature on the plate surface drops below 0.5 °C in 300 s of heating up.

If the time moment of steady state achievement depends on the rate of temperature change at the surface, there has to be a relationship between the time moment of steady state achievement and the heat sources depth.

Comparing numerically obtained steady-state temperature distributions of heating plates with different heat sources depths and the steady-state thermogram of the heating plate sample will provide the correct depth.

The numerically obtained steady-state temperature distributions for the heating plate over a range of heat sources depths are shown in Figure 8.

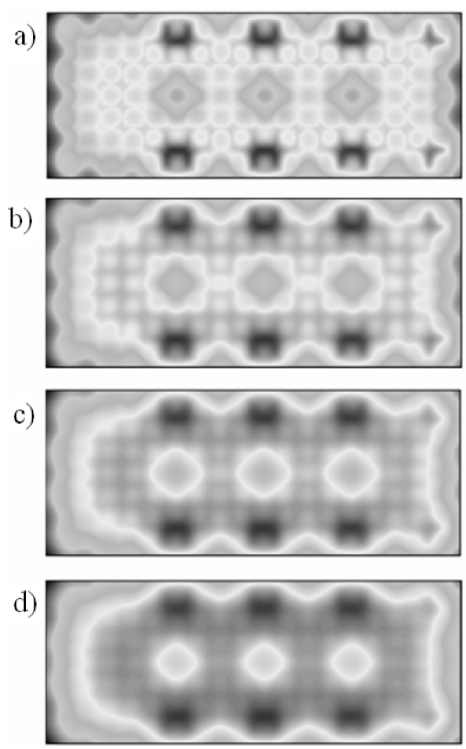

Figure 8. Numerically obtained temperature distributions of the heating plate at steady state for heat sources depth of: a) 5 mm, b) 7.5 mm, c) 12.5 mm and d) 17.5 mm

Slika 8. Numeričkim putem dobivene temperaturne raspodjele grijaće ploče uz dubinu izvora topline od: a) 5 mm, b) 7 mm, c) 12,5 mm and d) 17,5 m

Larger heat sources depth also supposes a thicker heating plate and a larger heat storage capacity. The heat sources locations can be easily identified from temperature distributions in Figure 8 a) and b). Contrary to them, temperature distributions in Figure 8 c) and d) do not look so clear any more because of a thicker stone layer. Thickening the material layer on the heat sources postpones the time moment of steady state achievement, as shown in Figure 9.

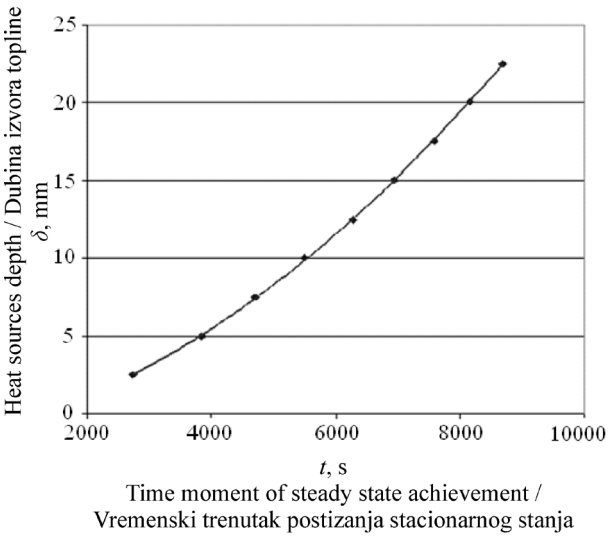

Figure 9. Time moment of steady-state achievement in dependence of heat sources depth

Slika 9. Ovisnost vremenskog trenutka postizanja stacionarnog stanja o dubini toplinskih izvora

For example, a heating plate with heat sources depth of 10 mm moves the steady state achievement to 5500 s of heating up and a heating plate with heat sources depth of 15 mm moves the steady state achievement to roughly 7000 s of heating up.

Thermographic measurements have been carried out for the heating plate sample and the resulting time moment of steady-state achievement is 6350 s. This value, from the plotted relationship on Figure 9, corresponds to a heat sources depth of 12.76 mm. According to the manufacturer, heat sources are buried in the heating plate midplane and thus giving the real depth of 12.5 mm. From the dependence between time moment of steady state achievement and heat sources depth, steady state conditions on the heating plate with heat sources depth of 12.5 mm are reached after 6270 s of heating up (Figure 8 c). The discrepancy between the measured and the real heat sources depth is about 2 %.

5.3. Influence of material properties

The time moment of steady state achievement has been studied numerically for different materials and different depths of heat sources, Figure 10. The properties of the heating plate materials are as in Table 2.

Stone and aluminium heating plates show pretty much the same dependence in Figure 10 and similar to them is a glass plate. The reason for that is a similar heat storage capability (the product of mass density and specific heat capacity) of the two. Cork as a material with poor heat storage capability precipitates earlier the moment of steady state and on the other side, steel postpones it.

Table 2.: Physical properties of cork, glass, steel and aluminium (Al)

Tablica 2. Fizikalna svojstva pluta, stakla, čelika i aluminija (Al)

	Cork/ Pluto	Glass/ Staklo	Steel/ Čelik	Al/Al
Thermal conductivity/ Koef. toplinske vodljivosti, W/m K	0.04	0.9	50	211
Density/ Gustoća, kg/m^3	150	3000	7850	2600
Spec. heat capacity/ Specifični toplinski kapacitet, J/kg K	1900	750	455	900

The numerically obtained temperature distributions for cork, glass, steel and aluminium heating plates at steady state and for a heat sources depth of 12.5 mm are shown in Figure 11. The four heating plates have equal heating output (roughly 800 W) at steady state, but show very different temperature distributions on the surface. Steel and aluminium, materials with high heat diffusivity, are characterized by a short temperature span on the surface. Cork and glass, low heat diffusivity materials show a large temperature span on the surface.

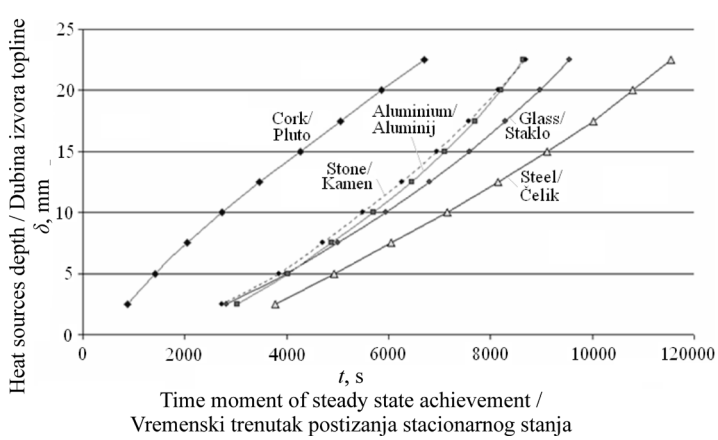

Figure 10. Time moment of steady state achievement as a function of heaters depth for 5 different plate materials

Slika 10. Vremenski trenutak postizanja stacionarnog stanja u funkciji dubine izvora topline za 5 materijala ploče

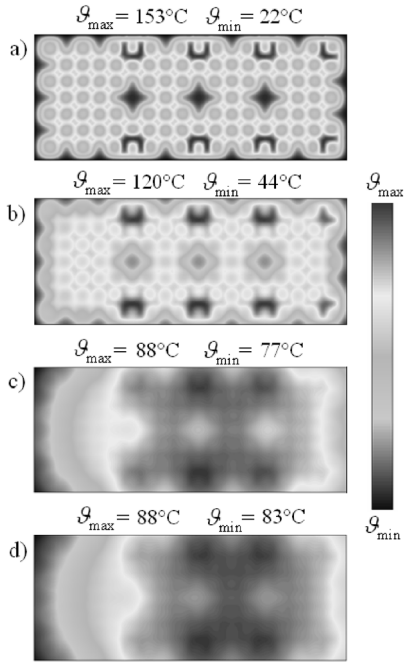

Figure 11. Steady-state temperature distributions for: a) cork, b) glass, c) steel and d) aluminium. The heat sources depth is 12.5 mm

Slika 11. Temperaturne raspodjele u stacionarnom stanju za: a) pluto, b) staklo, c) čelik i d) aluminij. Dubina izvora topline je 12,5 mm

Convection participates with 43 % and radiation with 57 % in the total heat transfer coefficient of the stone heating plate. Until steady state is achieved, only a part (about 65 %) of the heat flux coming from the heaters is delivered to the surroundings, the remaining heat is being stored in the plate as shown in Figure 13.

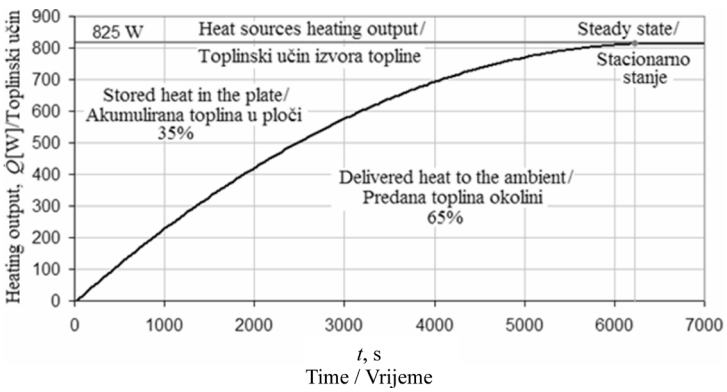

Figure 13. Transient heating output, stored and delivered heat of the stone heating plate. The heat sources depth is 12.5 mm and the time moment of steady-state achievement is 6350 s. Data calculated from thermograms

Slika 13. Toplinski učinak, akumulirana i predana toplina kamene grijaće ploče u ovisnosti o vremenu. Dubina izvora topline iznosi 12,5 mm, a vremenski trenutak postizanja stacionarnog stanja je 6350 s. Podaci dobiveni iz termograma

However, the average surface temperature for all the four heating plates, should be equal (about 86 °C), if an equal emissivity factor for all the four plates is assumed.

5.4. Total heating output of the plate

The average heat transfer coefficients for the stone heating plate are calculated from (6) and (7) using numerically obtained temperature distributions. Their values against time are shown in Figure 12.

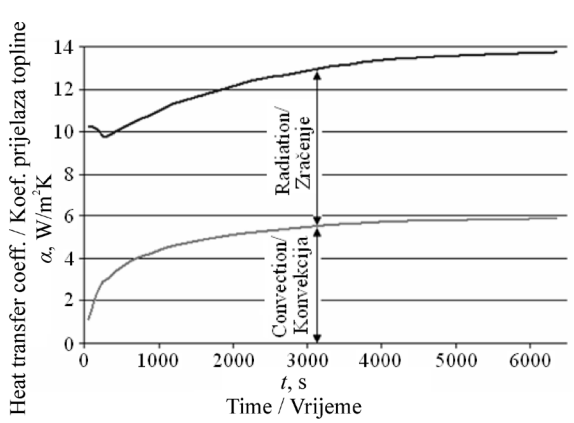

Figure 12. Convection and radiation in the total heat transfer coefficient of the stone heating plate

Slika 12. Udio konvekcije i zračenja u ukupnom koeficijentu prijelaza topline kamene grijaće ploče

According to thermographic measurements, the plate heating output in a steady state follows to be 825 W, which is in excellent accordance with the declared heating output of 800 W. The numerically obtained heating output is 770 W and the reason for the discrepancy is found in differences between average temperatures for the plate at steady state (Figure 4). The declared heating output is not reached until a steady state is achieved and by then the average heating output is 535 W. In other words, until a steady state is achieved, 35% of the heat sources heating output is being stored in the plate as accumulated heat.

The numerical analysis has been expanded to investigate the transient heating outputs for the five chosen materials of a heating plate with heat sources depth of 7.5 mm. The results are displayed in Figure 14. The steady-state heating output for a cork heating plate is reached quite early, i. e. after 2000 s of heating up. Heating plates having material properties such as aluminium, glass and stone reach the steady-state heating output approximately after 5000 s of heating up. The reason for that is found in similar heat storage capabilities of the three materials. On the other hand, steel as a material with higher heat storage capability delays the achievement of steady-state heating output.

Transient heating output for the stone heating plate with five different heat sources depths is shown in Figure 15. It is concluded that the larger the heat sources

depth the longer the time for steady-state heating output achievement.

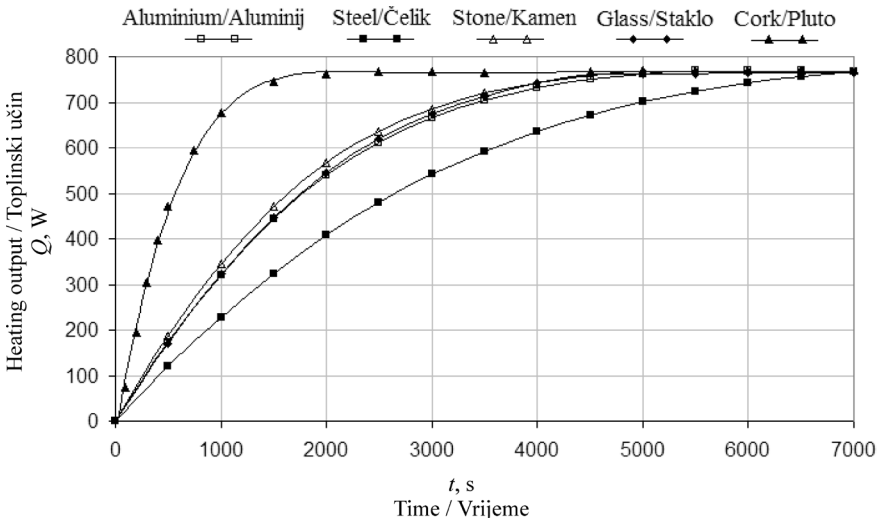

Figure 14. Transient heating output for heating plates having cork, steel, stone, glass and aluminium as the material. The heat sources depth is 7.5 mm. Data obtained from numerical analysis

Slika 14. Nestacionarni toplinski učinci grijaćih ploča od pluta, čelika, kamena, stakla i aluminija. Dubina grijača je 7,5 mm. Podaci dobiveni numeričkom analizom

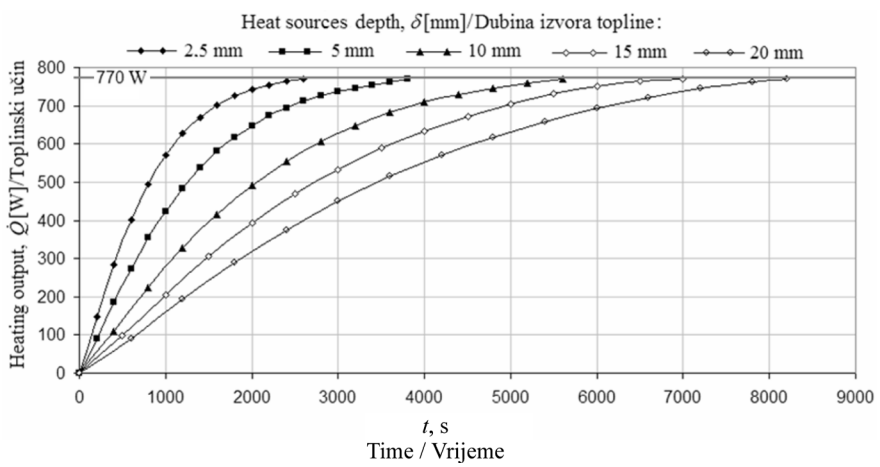

Figure 15. Transient heating output for the stone heating plate with five different heat sources depths. Data obtained from numerical analysis

Slika 15. Nestacionarni toplinski učinci za kamenu grijaću ploču za pet različitih dubina izvora topline. Podaci dobiveni numeričkom analizom

The last figures lead to a logical conclusion: if the heating plate is used as an ordinary room radiator supposed to warm up the ambient as fast as possible, the chosen material should be a low heat storage capability material and the heat sources depth, i. e. the plate thickness should be kept as small as possible.

If the heating plate is supposed to release the accumulated heat in the ambient for a longer period of time, the chosen material should be a high heat storage capability material and the heat sources depth, i. e. the plate thickness should be larger.

6. Conclusions

Combining thermographic and numerical approaches for the analysis of heat transfer inside and outside a heating plate with complex heat sources has been introduced as a powerful engineering apparatus.

The chosen numerical model proved to be successful in determining the transient temperature fields on the heating plate surface. Furthermore, the influence of material heat storage capability and the influence of heat sources depth on temperature fields and transient heating outputs have been studied. The ratios of convection and radiation in the overall heat transfer coefficient of the plate have been elaborated.

It has been concluded that attention should be given to the influence of plate thickness and material physical properties on the heating output of the heating plate in order to accommodate the duty requirements of the heating plate.

Acknowledgments

This research has been performed as a part of the scientific project *Research and Development of Renewable Energy Components and Systems*, supported by the Ministry of Science, Education and Sport of the Republic of Croatia.

REFERENCES

[1] CARLSLAW, H.S.; JAEGER, J.C.: *Conduction of Heat in Solids*, 2nd ed., Oxford University Press, London, 1959.

[2] ARPACI, V.S.: *Conduction Heat Transfer*, Addison-Wesley Publishing Company, Reading, 1966.

[3] BLECICH, P.: *Primjena Termovizijske Infracrvene Kamere u Termotehnici*, Diplomski rad, Tehnički fakultet, Rijeka, 2008.

[4] BEJAN, A.; KRAUS, A.D.: *Heat Transfer Handbook*, John Wiley & Sons, Hoboken, New Yersey, 2003.

[5] PATANKAR, S.V.: *Numerical Heat Transfer and Fluid Flow*, Taylor & Francis, New York, 1980.

[6] *Fluent V6.3 User Guide,* FLUENT Inc., Lebanon NH, 2006.

[7] VERSTEEG, H.K.; MALALASEKERA, W.: *An Introduction to Computational Fluid Dynamics: The Finite Volume Method*, Longman Scientific and Technical, Essex, England, 1995.

[8] ...: *ThermaCAM S65-User's Manual*, FLIR Systems, Publ. No. 1557990 Rev. a155, 2006.